Thomas Krummrein, Martin Henke, Peter Kutne, Manfred Aigner
Numerical analysis of operating range and SOFC-off-gas combustor requirements of a biogas powered SOFC-MGT hybrid power plant
Appl. Energy. 232 (2018) 598-606

The original publication is available at www.elsevier.com

http://dx.doi.org/10.1016/j.apenergy.2018.09.166

Numerical Analysis of Operating Range and SOFC-Off-Gas Combustor Requirements of a Biogas Powered SOFC-MGT Hybrid Power Plant

T. Krummrein*, M. Henke, P. Kutne, M. Aigner

German Aerospace Center, Institute of Combustion Technology, Pfaffenwaldring 38-40, 70569 Stuttgart, Germany

Abstract

Hybrid power plants which combine a micro gas turbine with solid oxide fuel cells, are projected to reach very high electric efficiencies. Powered by biogas, they have the potential to become an important pillar for a future CO_2-neutral energy mix. However, to compensate the fluctuating energy yield of wind turbines and photovoltaic power plants, they should also provide a wide operating range. While previous numerical studies show that this is the case for natural gas powered hybrid power plants, the impact of biogas utilization on the operating range is still unknown.

In the present study, a detailed numeric model of the hybrid power plant demonstrator being constructed at the DLR is presented. The model is used for an in-depth investigation of the operating limits using biogases with various methane contents. The influence of fuel cell operating limits, like the stack temperature, minimal cell voltage and maximal fuel utilization ratio, on the hybrid power plant operating range are discussed. While the results show a strong correlation between methane content and operating range, a power output reduction of 33 % is still feasible for methane contents as low as 60 vol%. Furthermore, knowing the operating range of the hybrid power plant is crucial for the design of the plant components. Therefore, in a final step, the operating conditions for the fuel cell off-gas combustor are derived for the respective operating ranges.

Keywords: Micro gas turbines, Solid oxide fuel cell, Hybrid power plant, Biogas, Operating range, Off-gas combustor

Nomenclature

Acronyms

DLR	Deutsches Zentrum für Luft- und Raumfahrt/German Aerospace Center
FU	Fuel Utilization
HyPP	Hybrid Power Plant
LHV	Lower Heating Value
MGT	Micro Gas Turbine
MGTS[3]	Micro Gas Turbine Steady State Simulator
SOFC	Solid Oxide Fuel Cell

Symbols

$c_{\Delta p}$	Pressure loss coefficient	$1/m^2$
$c_{\text{loss},\dot{Q}}$	Heat loss coefficient	W/K
I	Current	A
P	Power	W
p	Pressure	Pa
T	Temperature	K
U	Voltage	V
$\dot{m}$	Mass flow	kg/s
$\dot{Q}$	Heat flow	W
ρ	Density	kg/m^3

Subscripts

comp	Component
el	Electrical
mean	Mean value
surr	Surrounding
sys	System

1. Introduction

In the face of climate change and ever stricter regulations on CO_2-emissions, the need for CO_2-neutral energy sources is growing. While wind power and photovoltaics are paramount for a future environmental friendly energy mix, their volatility puts a strong burden on energy grids [1]. Due to of these fluctuations and ultimately the risk of dark doldrums, complementary power sources must be available [2]. Power plants

*Corresponding author

Email address: Thomas.Krummrein@DLR.de (T. Krummrein)

using biofuels can provide such a CO_2-neutral power source [3]. These power plants must provide a wide operating range to compensate for volatile renewable power sources. Additionally, sources of biomass that do not compete with food production like wood, industrial waste or landfill gas are scarce and their composition vary over time [4]. Thus, power plants should utilize these sources with high efficiency and must be able to handle the fluctuating calorific value of the fuels.

One promising candidate for such a biofuel-operated power plant is the combination of a micro gas turbine (MGT) with a solid oxide fuel cell (SOFC) module. In such a hybrid power plant (HyPP), the MGT pressurizes the SOFC module and thus increases its electrical efficiency or power output [5]. Furthermore, the hot SOFC-off-gas contains residual fuel which is burned in a downstream combustor. The gas is then expanded in the turbine to power the compressor and further increase the power output of the HyPP. As a result, HyPPs are projected to reach high electric efficiency. For example, Chan et al. simulated a HyPP with an electrical efficiency (LHV) of up to 62 % at an electrical output of about 2100 kW [6]. Additionally, Veyo et al. estimated an electric efficiency of 55 % for a 300 kW_{el} HyPP and also for a 220 kW_{el} HyPP [7]. Furthermore, Kaneko et al. predicted an electric efficiency of about 56 % for a HyPP with a design electric output of 35 kW_{el} [8]. Panne et al. simulated a HyPP based on a Turbec T100 MGT and reaches electrical efficiencies (LHV) above 55 % and an electric output of about 370 kW [9]. These simulations and predictions are further supported by experimental data: A proof-of-concept 220 kW_{el} HyPP with a Siemens-Westinghouse SOFC module reaches an electric efficiency of about 53 % [10]. Also, a Mitsubishi demonstration plant generates 200 kW_{el} output with an efficiency (LHV) of 54 % [11].

These studies show that in contrast to other power plants (e.g. combined gas and steam power plants), HyPPs achieve high efficiencies even at small electrical power outputs. The studies indicate that electrical efficiencies over 60 % for electrical outputs smaller than 100 kW_{el} are realizable. Hence, HyPPs can be employed decentralized. Furthermore, biogas power plants require thermal energy for the fermentation process. For a typical biogas plant in central Europe, the thermal energy is about 5 % to 15 % of the biogas energy [12], which is in the range of the usable heat of the HyPP exhaust gas. Therefore, a biogas powered HyPP may use most of the biogas energy without the need of the availability of additional heat consumers.

HyPPs also support a wide operating range relying on natural gas [13]. Whether the same can be achieved with biogas and whether HyPPs can handle the strongly fluctuating calorific value are decisive factors for the successful positioning of the technology in a future CO_2-neutral energy market. To resolve this concern and other related questions, the DLR institutes of Combustion Technology and Engineering Thermodynamics are conducting a collaborative effort in the EU Horizon 2020 project “Bio-HyPP” [14] to build a HyPP demonstrator. It combines a 3 kW_{el} MGT with SOFCs in planar design supplying 30 kW_{el}. Supporting this endeavor, detailed numerical process simulations are done to anticipate the impact of biofuels on the HyPP in construction.

It is often assumed that the fuel flexibility of SOFCs and MGTs can also be maintained by combining them into a HyPP. However, this aspect is not often mentioned in publications, especially the influences of low calorific fuels. Harun et al. from the National Energy Technology Laboratory used low calorific fuels in some HyPP real-time hardware-in-the-loop investigations. These investigations focus on sudden changes in fuel composition and the impacts to the transient behavior [15] and the SOFC [16], as well as the controlling of the HyPP during such maneuvers [17]. Fryda et al combined a biomass air gasification with a HyPP system in a numerical study [18]. The potential of a HyPP system for this application is compared with systems which contain either only an SOFC module or an MGT. Wongchanapai et al. investigated the use of biogas with 60 vol% methane in a HyPP [19]. Besides the reforming agent the fuel utilization factor, the turbine inlet temperature and the compression ratios were varied. Additionally, Kaneko et al. investigated a HyPP which is driven by a preheated fuel containing 40 % water, 35 % to 40 % methane and 25 % to 20 % carbon dioxide [8].

These studies focus on the design and specification of controllers (Harun [17, 15, 16] and Kaneko [8]) respectively HyPP systems (Fryda [18] and Wongchanapai [19]) for one or few specific fuels. However, the influence of fuels with strongly different calorific values in a certain power plant is not systematically investigated. The present study examines the use of such fuels in the DLR HyPP demonstrator, as well as the impact mechanisms of such fuels.

The present paper starts with a description of the HyPP demonstrator test rig, the steady-state simulation tool and the system model. This includes a discussion of boundary conditions and special characteristics of the model. While an overview of the HyPP operating range was given already at the EFC conference in 2017 [20], here the various mechanisms that limit operating range are described in more detail, again with an emphasis

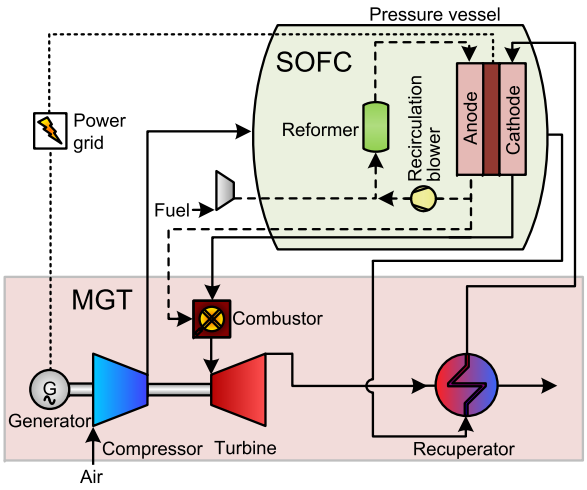

Figure 1: Structure of the HyPP demonstrator model [21].

on the impact of biogas composition. Building on this work, the requirements for the SOFC off-gas combustor are derived and presented for the entire operating range. Knowing the accurate boundary conditions of the combustion chamber is crucial in the design process, as they differ considerably from the conditions in a conventional MGT.

2. System Description

Figure 1 shows a simplified structure of the HyPP demonstrator which is currently being built at the DLR. It contains all components of the real demonstrator which are essential for steady state operation. First, ambient air is compressed with a maximum pressure ratio of approximately 3. The compressed air is then used to purge the pressure vessel which contains the SOFC stack. This ensures low pressure differences between the stack and the surrounding air. Furthermore, it prevents an explosive atmosphere in case of leakages. The purging air is then preheated with a recuperator which travers to the cathode of the SOFC module. The anode is supplied with a mixture of fuel and recirculated anode off-gas. The use of a recirculation blower allows to set the recirculation ratio. This system layout includes only one combustor which is used to burn the anode off-gas. Additionally, it can be supplied directly with fuel (not shown in Fig. 1) during the start up procedure or certain operating maneuvers. The hot exhaust gas from the combustion chamber is first expanded in the turbine which drives the compressor and the generator. It is then used to preheat the compressed air via the recuperator. The remaining energy of the exhaust gas can be utilized as a heat source. If a suitable heat consumer is available, about 20 % of the fuel energy can be reused in this way.

Most of the electric output is produced by the SOFC module with up to 30 kW_{el}. The main task of the MGT system is to provide high temperature and pressure air for the SOFC module. However, the high temperature exhaust gas from the SOFC off-gas combustor provides enough enthalpy for the turbine to not only power the compressor, but also to power a generator with a maximum output of approximately 3 kW_{el}.

3. Methodology and Model Description

3.1. Simulation Tool

The impact of biogas as fuel for a HyPP is investigated with a numerical steady state model of the HyPP demonstrator. The model is created with the in-house simulation tool *Micro Gas Turbine Steady State Simulator (MGTS^3)*. This is a modular simulation tool based on Matlab/Simulink with a library that contains a variety of 0D component models including several models for heat and pressure losses. This allows a highly flexible modeling of MGT based systems.

The MGTS^3 tool is based on the work of Panne et. al. [9], which introduced the fundamental component models like compressors and turbines. The tool was further developed and extended by Henke et. al. where more detailed component models for recuperators and water heat exchangers were introduced [22]. Also Henke et al. validated the simulation tool with measurement data from a Turbec T100 MGT and displayed the ability to represent MGT systems with high precision [23]. Furthermore, Krummrein et. al. implemented an improved solver routine, which enabled the detailed simulation of complex systems like HyPP [21].

In the MGTS^3 tool, all fluid flows are characterized by total temperature, total pressure, mass flow and composition of the flow. The calculation of gas flows assumes ideal gas mixtures with temperature depending polynomials [24] to calculate heat capacity and derived quantities.

The HyPP demonstrator model of this study contains 0D models for each component including the piping according to Fig. 1. The fixed quantities of this model are the operation conditions listed in Tab. 1 and the component parameters mentioned in the following sections. Take note that in the model configuration used here, the electric output of the system is not specified by the user. Instead, it correlates strongly with the user specified MGT shaft speed. Additionally, in contrast to various existing SOFC system analysis approaches, the fuel utilization is also not specified by the user, but determined

Quantity	Value
Stack temperature	1073 K to 1123 K
MGT shaft speed	150 krpm to 240 krpm
Fuel methane content	40 vol% to 100 vol%
Ambient temperature	288 K
Ambient pressure	1013 hPa
Fuel inlet temperature	288 K
Turbine outlet temp.	1060 K
Recuperator efficiency	90 %
Recirculation ratio	80 %

Table 1: Operating conditions used in the HyPP model.

by the operating conditions. This will be described in more detail in the next section.

Lastly, to give a brief overview of the system, Tab. 2 lists some results of the model for two reference steady state cases.

3.2. Heat and Pressure Losses

With the exception of compressor and turbine, all flow component models consider heat and pressure losses. Heat losses are assumed to be proportional to the temperature difference of the components mean temperature and the temperature of the surrounding [21]:

$$\dot{Q}_{\text{loss}} = c_{\text{loss},\dot{Q}} \cdot \left(T_{\text{comp,mean}} - T_{\text{surr}}\right) \tag{1}$$

Here T_{surr} is the surrounding temperature of the component. This is the mean vessel temperature for the components inside the pressure vessel and the ambient temperature for all other components. Additionally, the proportionality constants $c_{\text{loss},\dot{Q}}$ are set in accordance with the heat losses at nominal conditions in the work of Steilen et. al. [13].

Furthermore, pressure losses are calculated with a simplified Darcy-Weisbach equation assuming a constant friction factor [21]:

$$\Delta p = c_{\Delta p} \cdot \frac{\dot{m}^2}{\rho} \tag{2}$$

The proportionality constant $c_{\Delta p}$ for the recuperator is calculated from manufacturer data. Since no measurement data is available, the pressure loss coefficients for the other components are calculated from design pressure losses based on experience.

3.3. Component Models

In the following, a brief overview of the most important components and their simulation models is given.

SOFC Stack. The SOFC stack model is a 0D model for planar SOFCs, which is developed and parameterized with experimental data by the DLR institute of Engineering Thermodynamics. The model assumes that the outlet flows of the SOFC module are in chemical equilibrium and that the temperatures are equal to the stack temperature. The chemical equilibrium is calculated with the Software Cantera.

It is assumed that the electric power can be converted with an efficiency of 95 %.

Turbomachinery. The compressor and turbine are modeled by turbo maps that have been determined experimentally. These maps provide the isentropic efficiency and pressure ratio for all relevant operating points depending on the reduced shaft speed and the reduced mass flow.

Friction losses of the shaft are described by a linear function of the shaft speed, which is based on manufacturer data. The efficiencies of the generator and the power electronics are assumed to be constant at 92 % and 94 % respectively.

Recuperator. The recuperator is calculated with a constant efficiency. It is the most critical component of the HyPP in terms of temperature and therefore, the turbine outlet temperature is limited by the maximum recuperator temperature. However, a decreasing turbine outlet temperature always influences the system negatively in terms of system efficiency and operating range. Therefore, the turbine outlet temperature in this study is specified as a constant boundary condition, which is set to its maximum value of 1060 K.

Reformer. In principle, the SOFC module is able to reform the hydrocarbons in the fuel itself. However, the additional reformer ensures that coking does not occur for all operating conditions. The reformer model uses an isenthalpic reforming process considering heat and pressure losses. The model assumes chemical equilibrium at the outlet which is calculated with the software Cantera.

Recirculation and Recirculation Blower. A high recirculation of SOFC anode off-gas is advantageous to reduce temperature gradients and allow for lower single pass fuel utilization ratios. However, very high recirculation ratios impose technical difficulties. Therefore, in this study a constant recirculation ratio of 80 % is used, where the recirculation ratio is defined as the quotient of the recirculated mass flow and the anode off gas mass flow. However, as many technological limitations apply,

Quantity	Case 1	Case 2
Operating conditions (see also Tab. 1):		
Stack temperature	1123 K	1123 K
MGT shaft speed	240.0 krpm	183.2 krpm
Fuel	Methane	40 vol% CH_4, 60 vol% CO_2
Exemplary quantities of steady state:		
El. output of system	36.9 kW	26.7 kW
El. efficiency of system (LHV based)	61.8 %	59.7 %
El. output of SOFC module (including conversion losses)	33.6 kW	25.5 kW
El. output of MGT (including conversion losses)	3.87 kW	1.87 kW
Air mass flow	50.9 g/s	29.4 g/s
Fuel mass flow	1.19 g/s	4.57 g/s
Compressor pressure ratio	3.09	2.06
Compressor isentropic efficiency	73.7 %	73.1 %
Turbine isentropic efficiency	76.5 %	75.9 %
Rel. pressure loss between Compressor and Turbine	6.8 %	5.1 %
Compressor outlet temperature	436 K	378 K
Vessel outlet temperature	482 K	469 K
SOFC module inlet temperature (air)	970 K	946 K
Turbine inlet temperature	1254 K	1178 K
Heat losses of components in pressure vessel (rel to fuel LHV flow)	5.1 %	7.1 %
Heat losses to ambient (rel to fuel LHV flow)	8.6 %	11.0 %

Table 2: Predicted values of relevant system quantities of HyPP for two exemplary cases.

the optimal value must be determined in future experimental studies.

An estimation of the recirculation system pressure losses is difficult, as well as the estimation of the recirculation blower behavior. Therefore, in this study, the recirculation blower is not considered. This is a conservative assumption with regard to the operating range, as the energy input of the blower is neglected. However, it is an optimistic assumption in terms of electric power output and efficiency of the system. It is expected that for natural gas as the fuel, the electric power of the recirculation blower is below 0.5 % of the electric output of the system.

Fuel Gas Compressor. The fuel gas compressor is calculated with a constant isentropic efficiency of 70 % and an electric drive efficiency of 90 %. However, the fuel temperature is not increased by the compression in this model. This is a conservative assumption to respect heat losses of the fuel supply system. In this study, the electric power of the fuel compressor is below 1 % of the electric output of the system for pure methane as fuel and between 1 % to 3 % for a fuel with 40 vol% methane.

4. Influence of Biogas on the HyPP System

The steady state HyPP model is used to investigate the influence of biogas quality on the system. The biogas is modeled as a mixture of methane and carbon dioxide, with methane contents between 40 vol% and 100 vol%.

4.1. Relations between electric output, stack temperature and SOFC system FU

An important quantity to explain the behavior of the HYPP system is the SOFC system fuel utilization (FU). This is the FU of the SOFC module including recirculation. Figure 2 shows the SOFC system FU for two stack temperatures and different methane concentrations of the fuel, dependent on the electric output of the system. In general, the SOFC system FU increases with decreasing power output. This is a result of the fixed turbine outlet temperature with also fixed SOFC stack temperature. Figure 3 explains the trend by looking at the distribution of the fuels energy to the SOFC system and the combustor when the electric power of the SOFC system changes. Also, the SOFC system FU increases with increasing stack temperature. According to

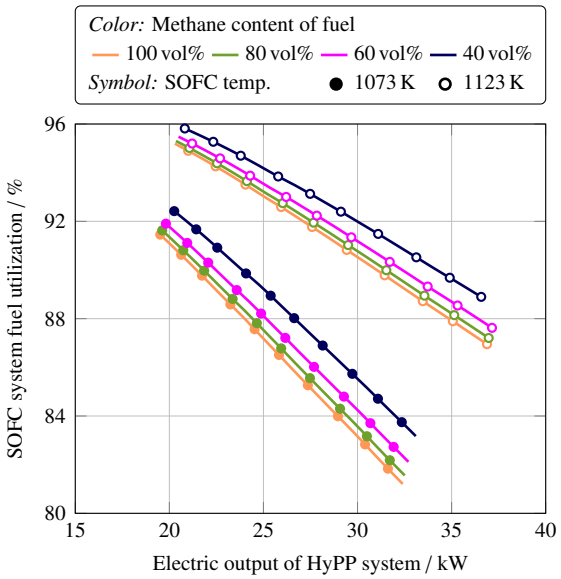

Figure 2: SOFC system fuel utilization of the SOFC module.

the explanation of Fig. 3, this is because of the decreasing $\dot{Q}_{\text{Combustor}}/\dot{Q}_{\text{SOFC}}$ ratio.

4.2. Impact Mechanisms of Biogas

An increasing proportion of carbon dioxide in the fuel influences the system via two mechanisms: First, the carbon dioxide increases the heat capacity flow of the fuel and, therefore, cools down the SOFC module. This must be compensated by a reduced air flow to maintain a certain stack temperature. The effect is further enhanced as the fuel enters the SOFC system with approximately ambient temperature whereas the inlet air temperature is approximately 950 K.

Secondly, the additional carbon dioxide decreases the Nernst potential at the SOFCs, as it increases the concentrations of a reaction product [25]. The effect is further amplified by the reduced air flow, which increases the oxygen utilization of the air and, therefore, reduces the oxygen partial pressure.

Both mechanisms increase the SOFC system FU which can be seen in Fig. 2. Further investigations of the model indicate that the impact of the cooling mechanism is stronger than the impact of the Nernst voltage decrease.

While the impact of these effects on the FU are clearly visible in Fig. 2, the influence e.g. on air mass flow is very low and hence, the impact of electric output variation is much stronger.

4.3. HyPP Process Quantities Limitations

An important question regarding the use of biogas in a HyPP is the influence on the operating range. It is determined by several limits of process quantities [13]:

- A maximum single pass fuel utilization ratio of 70 % prevents fuel starvation and increased degradation of the SOFC cells.
- The SOFC cell voltage must be above the nickel oxidation limit. Including a safety margin, the limit is set to 0.68 V.
- An exceedingly large oxygen utilization of the air can lead to cell degradation. Therefore, it is limited here to 50 %.
- The ceramic components of the SOFCs must be protected against large spatial temperature gradients. Therefore, in accordance with the supplier, the temperature difference between the anode and cathode inlet must be below 150 K, between the stack core and the anode inlet below 300 K and between the stack core and the cathode inlet below 250 K. As the SOFC module is represented by a 0D-model, the conservative assumption is made that stack core temperature is equal to stack outlet temperature.
- In accordance with the manufacturer, the stack core temperature for steady state operations must be between 1073 K and 1123 K.
- The shaft speed of the MGT must not exceed the maximum manufacturer value of 240 000 rpm.
- As described before, the turbine outlet temperature must not exceed the maximum recuperator temperature of 1060 K.

In the following sections, these operating limits are investigated for biogases with different methane contents as fuel. The analysis is performed for stack temperatures of 1073 K and 1125 K to highlight the impact of stack temperature variation and the operating limits caused by stack temperature limits.

4.3.1. Single Pass Fuel Utilization

Figure 4 shows the single pass FU of the SOFCs for a recirculation ratio of 80 %. For a constant recirculation ratio, the relation between the SOFC system FU and the single pass FU is monotonous. Therefore, the behavior of the single pass FU is very similar to the SOFC system FU described above. It can be seen that for high stack

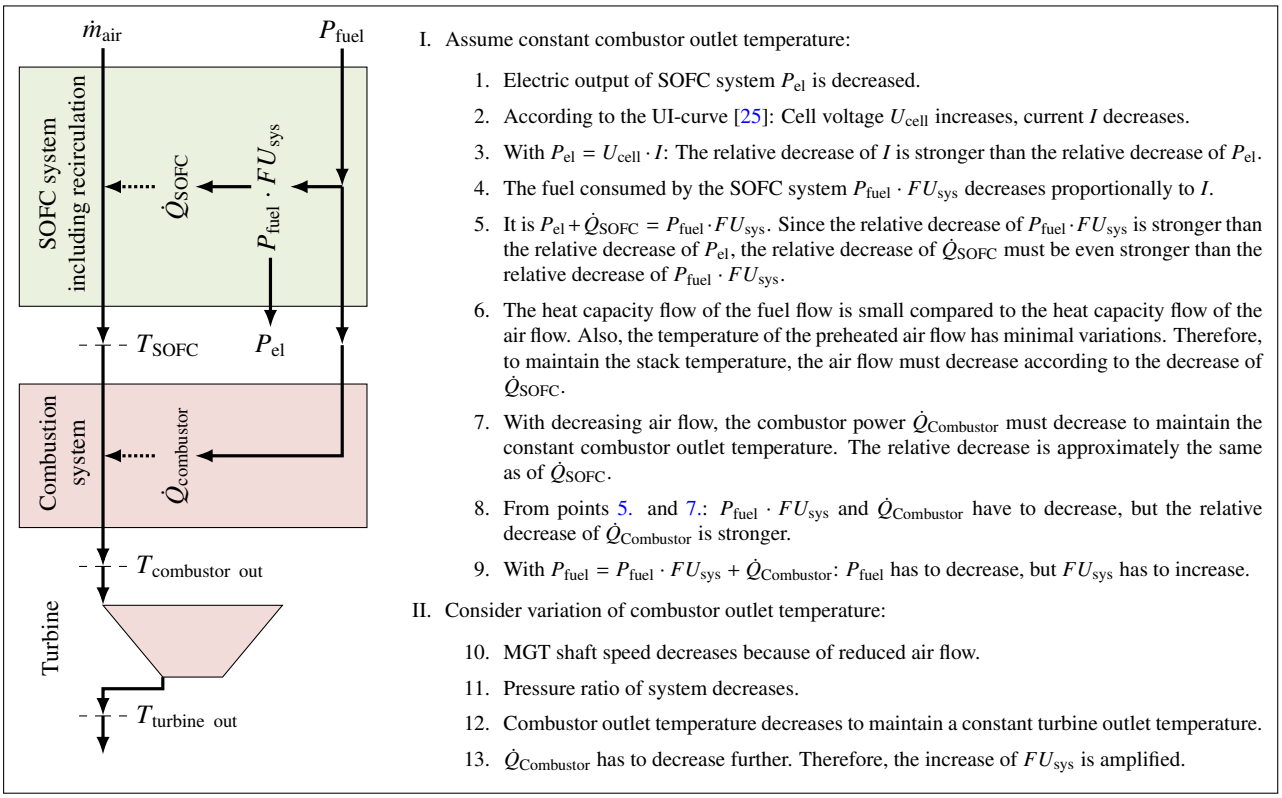

Figure 3: Derivation of decreasing SOFC system FU with decreasing electric power output at constant stack and turbine outlet temperature. The heat capacity of the fuel is neglected.

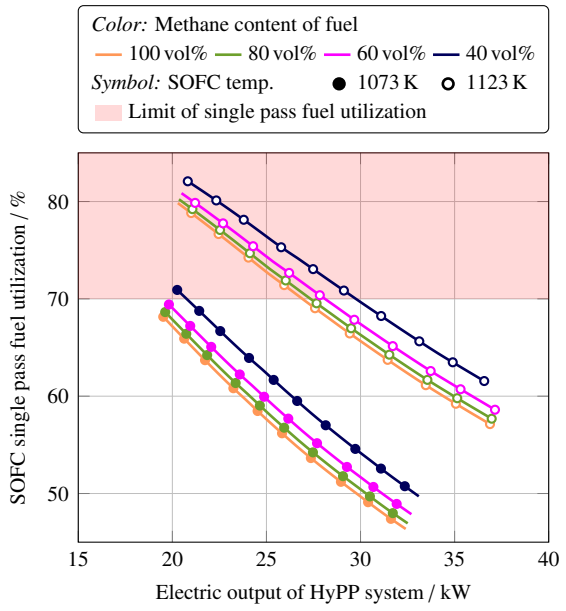

Figure 4: Single pass fuel utilization of the SOFCs at a recirculation ratio of 80 %.

temperatures and low electric output, the single pass fuel utilization limit is exceeded. It is possible to reduce the single pass fuel utilization, maintaining the SOFC system fuel utilization, by increasing the recirculation ratio. However, this is only possible within certain limits, since an excessive recirculation ratio causes excessively large pressure drops and pressure differences, as well as being technically impracticable. Therefore, in the following, the recirculation ratio will remain at a constant value of 80 %.

Analogous to the investigation of the SOFC system FU, increasing carbon dioxide content of the fuel increases the single pass fuel utilization only slightly. Again, Fig. 4 shows that the effect is minor in comparison to the electric output variation over a typical operating range.

4.3.2. Oxygen Utilization

As described above, the cooling effect of the additional carbon dioxide in the fuel results in a lower air mass flow and, therefore, an increased oxygen utilization. In contrast to the rather small effect on FU, oxygen utilization x changes over the methane content range to

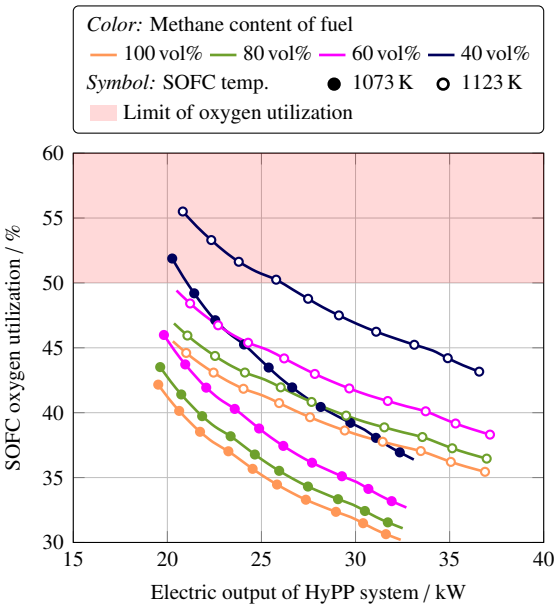

Figure 5: Oxygen utilization of the SOFCs.

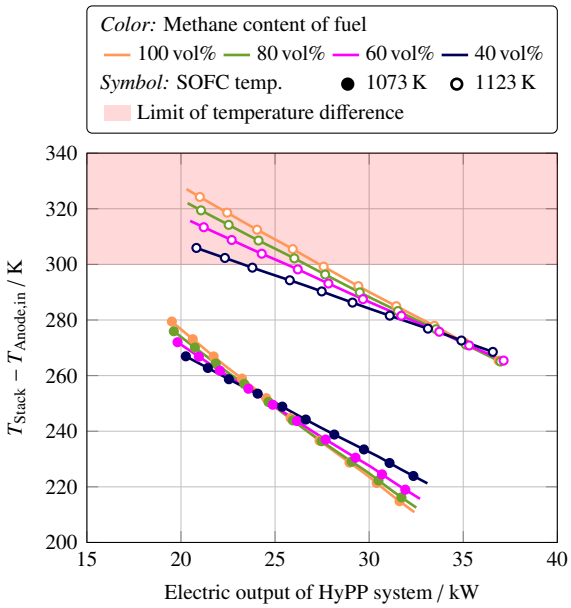

Figure 6: Temperature difference between stack and anode inlet at a recirculation ratio of 80 %.

a similar magnitude as over the electrical power range.

Figure 5 shows that the air utilization for a fuel with 40 vol% methane content is increased by approximately 25 %, compared to pure methane. Additionally, for methane lean fuels, the air utilization limit is exceeded for low electric outputs.

4.3.3. SOFC Temperature Differences

The mixture of recirculated anode off-gas and fuel is reformed before the anode inlet. The reforming process reduces the methane content of the anode inlet flow to avoid coking. However, the endothermic process also reduces the temperature, in particular for low anode mass flow rates at small recirculation ratios.

Figure 6 shows that with a stack temperature of 1123 K and pure methane, the maximum temperature difference between the stack core and the anode inlet flow is exceeded below a critical electric output of approximately 27 kW. Lower stack temperatures reduce the critical electric output significantly. The fuel composition has only a very small impact on the critical electric output, however, methane lean fuels show a slightly decreased critical electric output.

The trend of the temperature difference between the stack core and the cathode inlet flow is similar to the trend of the temperature difference between stack core and anode inlet. However, even for small electric outputs and high stack temperatures this temperature difference is more than 50 K below its limit. Furthermore, the temperature difference between the anode and the cathode inlet flows does not exceed its limit in any of the cases examined.

4.3.4. MGT Shaft Speed

The MGT shaft speed determines the air mass flow and the pressure ratio of the system. Therefore, low stack temperatures and large electric outputs increase the shaft speed. The maximum electric output of the HyPP demonstrator is reached at the maximum shaft speed of 240 000 rpm. Figure 7 shows that for a stack temperature of 1123 K, the maximum is about 35 kW. The cooling effect of carbon dioxide in the fuel results in a slightly reduced air mass flows. Therefore, the shaft speed for methane lean fuels is slightly decreased. Again, the impact of fuel composition variation is small compared to the impact of a variation in electric output.

4.3.5. SOFC Cell Voltage

Compared to the previous examples, the reduction of SOFC cell voltage, due to decreasing fuel methane content, has the most significant implication on the HyPP operating range. While a reduction of methane content to 80 vol% does not reduce the operating range, Fig. 8 depicts that further reductions lead to an overproportional voltage drop and a narrowing of operating limits. Additionally, take note that the sensitivity of the methane content is more pronounced than the sensitivity of the electric output on cell voltage.

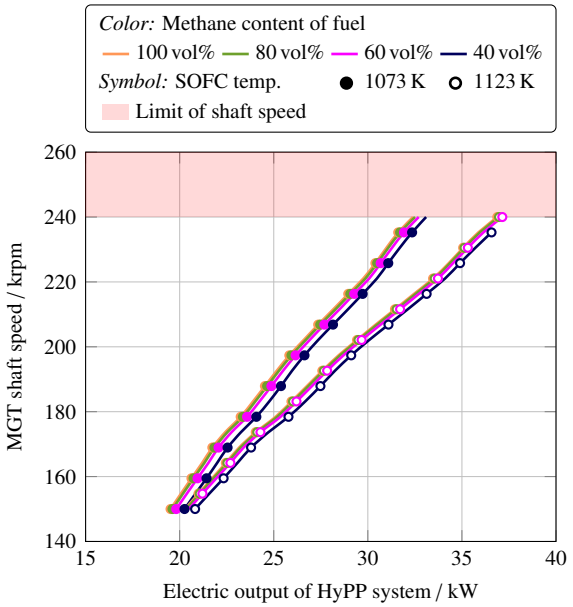

Figure 7: Shaft speed of the MGT.

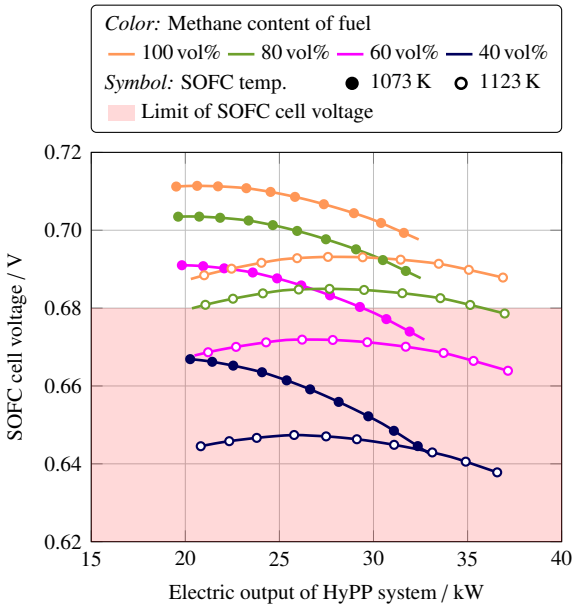

Figure 8: Cell voltage of the SOFCs.

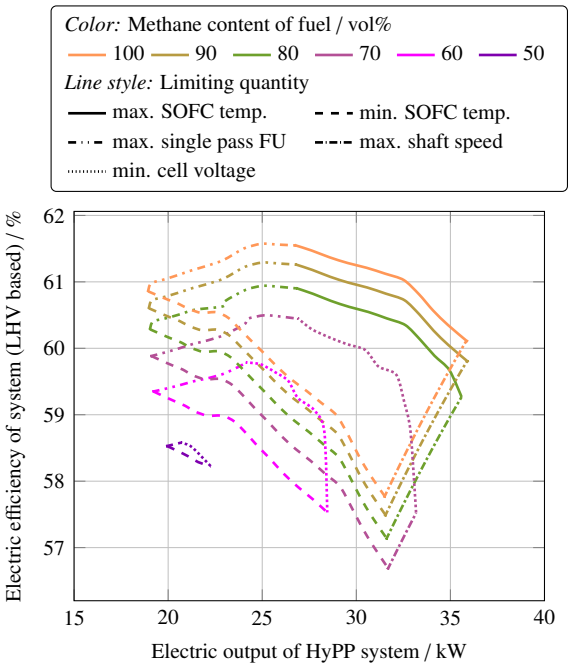

Figure 9: Operating range for the HyPP demonstrator for different methane concentrations of the fuel and a recirculation ratio of 80 % (Recirculation blower is not taken into account).

A slight reduction in the minimal SOFC cell voltage limit below 0.68 V may be acceptable. However, an investigation of the related trade-off is not a topic of this study.

4.4. System Operating Range

Figure 9 summarizes the behavior of the quantities described in the previous section to the expected operating range of the HyPP demonstrator. It displays the overall electric LHV-based efficiency of the system versus the electric output.

The different colored lines express the different methane concentrations of the fuel, while the different line types determine the most limiting quantity. It can be seen that the oxygen utilization and the stack temperature differences have no impact on the operating range. Furthermore, for methane rich fuels, the SOFC cell voltage limit is no restriction. For these fuels, the operating range is limited towards large electric outputs by the maximum shaft speed and the maximum stack temperature. For small electric outputs, the operating range is limited by the maximum single pass fuel utilization and the minimum stack temperature.

However, with decreasing methane concentration of the fuel, the maximum stack temperature limit and the fuel utilization limit are replaced by the cell voltage

limit as the most restrictive quantity. This results in a substantial reduction of the operating range. As described above, for methane contents below approximately 50 vol% operation is not possible considering the defined limits.

The impact of fuel methane concentration to the relevant thermodynamic properties of the system is rather small. Therefore, the impact to the system efficiency is also small, as shown in Fig. 9. With a methane concentration of 80 vol%, the maximum reachable electric efficiency decreases by approximately 0.6 percentage points compared to pure methane.

As a lower cell voltage limit might be possible, a small study was performed to investigate the performance with a methane content of 40 vol%, neglecting the fuel cell voltage limit. In this case, system efficiency at a stack temperature of 1123 K decreases by approximately 3.5 percentage points in comparison to pure methane.

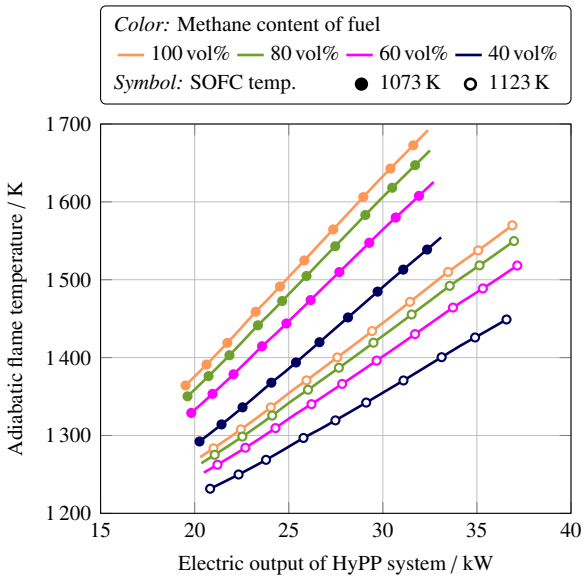

Figure 10: Adiabatic flame temperature of combustin with an cathode off-gas split of 20 %.

5. Influence of Biogas on the Combustion System

The previous section explains that the methane content of the fuel only slightly influences most thermodynamic process variables of the HyPP. However, some of the variables change significantly, which includes the combustion chamber inlet. Therefore, the impact of biogas on the combustion system is investigated. Furthermore, the SOFC off-gas combustion system must be able to burn fuels with a very low calorific value. Therefore, it can be expected that the combustion chamber causes further limitations to the operating range. Indeed, preliminary experiments with natural gas as fuel confirm this for the initial combustor design, which is used in the DLR HyPP demonstrator: It probably reduces the operating range of Fig. 9 further for low electric outputs. However, further experiments are needed to understand this limitation more precisely. Therefore, this section focuses on the general requirements of the combustion chamber in a HyPP supplied with biogas.

The heat capacity of carbon dioxide and air or exhaust gas is almost the same. Therefore, the decrease of air mass flow caused by the increasing concentration of carbon dioxide in the fuel is approximately equal to the additional fuel carbon dioxide mass flow. Thus, decreasing the methane content of the fuel from 100 vol% to 40 vol%, with fixed electric output, reduces the combustion chamber outlet mass flow by less than 5 %. Additionally, the heating power of the combustion system is reduced by about 10 %, while the combustion chamber outlet temperature changes by less than 5 K.

However, while the conditions at the combustion chamber outlet are only slightly affected by the use of biogas, the impact on the inlet conditions is stronger. In a typical MGT/HyPP combustion system, only a section of air is used for the actual combustion process while the larger mass of air is mixed downstream with the combustion exhaust gases. The percentage of air that will be used in the combustion reactions is described by the ”off-gas split” value. A lower off-gas split allows for higher adiabatic flame temperatures and, therefore, more stable combustion, while maintaining the temperature limits of the combustion system outlet. Therefore, the cathode off-gas split is an important combustion system design quantity to achieve stable combustion with low emissions.

Figure 10 depicts the adiabatic flame temperature at an exemplary cathode off-gas split of 20 %. Remarkably, the adiabatic flame temperatures are quite low: In a conventional MGT process with biogas, a combustion chamber with the same air split value will reach adiabatic flame temperatures between 1900 K and 2250 K. This trend is due to the high heating value of the biogas compared to the very low heating value of the SOFC anode off-gas. Combustion systems for methane supplied HyPP exist. However, while the adiabatic flame temperatures are significantly low for methane utilization, an additional decrease due to the use of biogas may make an adjustment of the off-gas split unavoidable.

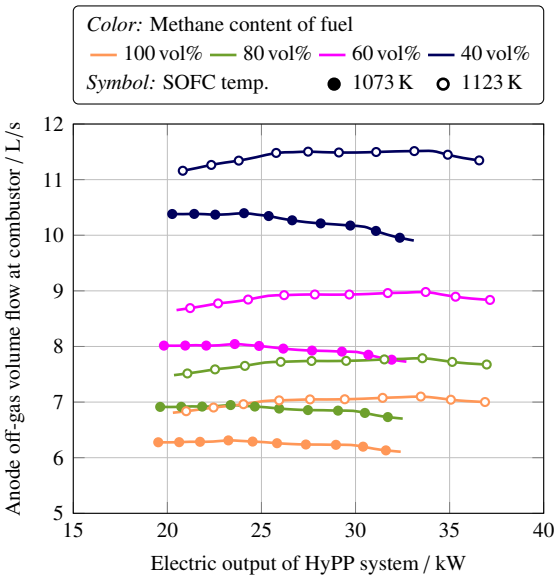

Figure 11: Volume flow of anode off gas to combustion chamber.

In the combustor, the fuel flows through nozzles to achieve a higher momentum. Figure 11 shows, that decreasing the methane content of the fuel can increase the anode off-gas volume flow up to approximately 65 %. Too low volume flows can result in instable combustion, while exceedingly large volume flows result in large pressure drops, which can lead to intolerable pressure difference between the SOFC anode and cathode. Therefore, it seems rather difficult to use the same nozzle number and geometry with methane lean fuels as well as with methane rich fuels. However, this functionality may be achieved by a more complex staggered combustion system.

Summarized, the combustion chamber inlet conditions for biogas utilization differs significantly from the conditions with pure methane as fuel in terms of absolute numbers, but significantly less with stack temperature or system power output variations. Therefore, it seems plausible that a HyPP combustion system, which works with methane rich fuels, can be easily adapted to a fuel with a lower methane content. However, to design a combustion system which works well with methane rich and lean fuels may impose a much larger challenge.

6. Discussion of Simulation Results

The simulation results presented in the previous sections are based on a model for a planned HyPP demonstrator. Therefore, one should discuss the results are reliable and whether they can be transferred to a real application.

The main parameters of most of the component models are either based on measurement data or on manufacturer data. Therefore, it can be expected that the computations of the components are not prone to error. However, the parameters for heat and pressure losses are based on estimations or experience values. Sensitivity studies show that the impact of increased pressure losses is quite small, while the heat losses of some components could have a noticeable impact (see also Steilen et. al. [13]) and could influence the operating range. Furthermore, some of the mentioned operating limits are based on experience. Further experiments are necessary to specify these limits more precisely, taking into account safe operation and the SOFC lifetime. Additionally, the operating limits of the combustion system are yet not available, however, at least for the initial combustor, an impact on the operating range is expected.

In general, a large operating range for SOFC/MGT HyPPs is assumed. In contrast, the operating range of Fig. 9 seems to not be remarkably large. However, it must be considered that this is the expected operating range of a demonstration plant. Therefore, it is not only influenced by the uncertainties described above, but also by scaling effects, such as large relative heat losses. Furthermore, an additional heat transfer to the SOFC module inlets from a suitable position between SOFC outlet and turbine inlet could be considered. While this increases the complexity of the system, it decreases the fuel utilization significantly (see Fig. 3) and, therefore, increases the SOFC cell voltage and the heating value of the SOFC off-gas.

The steady state simulations with biogas result in two main findings: First, the use of biogas does not strongly influence the majority of thermodynamic quantities of the HyPP, including the system efficiency. In particular, the relative impacts are small compared to the relative variation of methane content. The reasons for this are discussed in the previous sections, the most important one being that the additional amount of inert species in the fuel is compensated by a slightly reduced air flow. However, the second finding is that a few of the relevant HyPP quantities do not follow the first statement. Therefore, these quantities must be carefully investigated if biogas is used as the fuel in a HyPP: The SOFC cell voltage decreases and, therefore, the nickel oxidation limit may be reached. This is mainly caused by the additional carbon dioxide on the SOFC anode, while simultaneously the oxygen utilization of the SOFC cathode increases. Therefore, the Nernst potential and the

cell voltage of the SOFCs decrease. Since these are general mechanisms, the decrease of the cell voltage for methane lean biogases is also a general aspect. However, the actual decrease in a certain application depends on many parameters and must be determined specifically. Because of the negative slope of the UI-curve, the decrease of the cell voltage for the same power output is larger if the absolute value for the reference case is already small.

The anode off-gas volume flow is another quantity which is strongly influenced by the biogas composition. Therefore, the design of the combustion system must fit the expected biogas composition. Another aspect which is not discussed in this study is the pressure loss of the SOFC anode, including recirculation and fuel supply, which will increase due to the increased volume flow.

Summarized, this study shows that the use of biogas in a HyPP has only significant impacts on the few mentioned quantities. As long as these impacts are considered, it can be expected that most of the knowledge about the operation of a HyPP with methane rich fuels can be transferred to the operation with biogas fuels.

7. Conclusions and Outlook

This paper investigates the impact of the use of biogas fuel for the DLR hybrid power plant demonstrator, which is a combination of a solid oxide fuel cell (SOFC) system and a micro gas turbine. A numerical steady state model is built with the MGTS^3 simulation tool which is used to identify and discuss several impact mechanisms. It is discussed that some of these impacts limit the operating range of the system. The influence of biogas is analyzed using fuel with methane concentrations between 40 vol% and 100 vol%.

The results show that the general thermodynamic process values and the SOFC electric efficiency are only slightly influenced by the change from methane to biogas. Therefore, at the same operating point in terms of stack temperature and electric system output, the electric efficiency of the system with a 40 vol% methane fuel decreases only approximately 3.5 percentage points (based on lower heating value) compared to pure methane as fuel. However, methane lean biogases strongly influence some of the system quantities. An important example is the decrease of the SOFC cell voltage: For methane concentrations below about 50 vol% it falls below its minimum limit of 0.68 V for all operating points. Furthermore, fuels with methane concentrations below approximately 80 vol% reduce the operating range significantly. The reduction is caused by several mechanisms that are described in detail.

In addition, the general impact of biogas on the off-gas combustion system is investigated. The increased amount of inert gases in the anode off-gas, as well as the reduced oxygen concentration in the cathode off-gas must be considered in the combustion system design. The simulation indicates that a stable combustion for all investigated fuel methane contents is realizable. However, the combustion chamber must probably be designed for a more narrow range of methane content than the investigated one. It seems challenging to design a single combustion chamber that is suitable for all methane concentrations ranging from 40 vol% to 100 vol%.

The hybrid power plant demonstrator currently being built at the DLR will be used in future work to validate the simulation model. This work will also show whether the minimum cell voltage limit can be further reduced without a heavy impact on SOFC degradation, to allow for lower methane content. Additionally, further research is being conducted in the field of the combustion system. The stability range of methane content variations and possibly also adapted combustion system designs. Additionally, further research will investigate the combustion system. This includes the stability range for methane content variations and, if necessary, adaptions of the combustion chamber design.

8. Acknowledgments

The authors would like to thank their colleagues in the DLR Institute of Engineering Thermodynamics for many fruitful discussions and support. Special thanks also go to Mike Steilen for providing the SOFC stack model, Timo Lingstädt for his valuable comments on the combustion system, as well as the whole DLR Bio-HyPP project team for their support.

This project has received funding from the European Union's Horizon 2020 research and innovation programme under grant agreement No 641073 (www.bio-hypp.eu).

References

[1] M. Anvari, G. Lohmann, M. Wächter, P. Milan, E. Lorenz, D. Heinemann, M. R. R. Tabar, J. Peinke, Short term fluctuations of wind and solar power systems, New Journal of Physics 18 (6) (2016) 063027.

[2] C. Zöphel, S. Schreiber, T. Müller, D. Möst, Which flexibility options facilitate the integration of intermittent renewable energy sources in electricity systems?, Current Sustainable/Renewable Energy Reports (2018) 1–8.

[3] N. Szarka, F. Scholwin, M. Trommler, H. F. Jacobi, M. Eichhorn, A. Ortwein, D. Thrän, A novel role for bioenergy: A flexible, demand-oriented power supply, Energy 61 (2013) 18–26. doi:10.1016/j.energy.2012.12.053.
URL https://doi.org/10.1016/j.energy.2012.12.053

[4] D. Deublein, A. Steinhauser, Biogas from waste and renewable resources: an introduction, 2nd Edition, Wiley-VCH, Weinheim, Bergstr, 2011, uB Vaihingen.
URL http://swbplus.bsz-bw.de/bsz330789473cov.htm

[5] M. Henke, C. Willich, C. Westner, F. Leucht, R. Leibinger, J. Kallo, K. A. Friedrich, Effect of pressure variation on power density and efficiency of solid oxide fuel cells, Electrochimica Acta 66 (2012) 158–163. doi:10.1016/j.electacta.2012.01.075.
URL https://doi.org/10.1016/j.electacta.2012.01.075

[6] S. Chan, H. Ho, Y. Tian, Modelling of simple hybrid solid oxide fuel cell and gas turbine power plant, Journal of Power Sources 109 (1) (2002) 111–120. doi:10.1016/s0378-7753(02)00051-4.
URL http://dx.doi.org/10.1016/S0378-7753(02)00051-4

[7] S. E. Veyo, L. A. Shockling, J. T. Dederer, J. E. Gillett, W. L. Lundberg, Tubular solid oxide fuel cell/gas turbine hybrid cycle power systems: Status, Journal of Engineering for Gas Turbines and Power 124 (4) (2002) 845. doi:10.1115/1.1473148.
URL https://doi.org/10.1115/1.1473148

[8] T. Kaneko, J. Brouwer, G. Samuelsen, Power and temperature control of fluctuating biomass gas fueled solid oxide fuel cell and micro gas turbine hybrid system, Journal of Power Sources 160 (1) (2006) 316–325. doi:10.1016/j.jpowsour.2006.01.044.
URL http://dx.doi.org/10.1016/j.jpowsour.2006.01.044

[9] T. Panne, A. Widenhorn, J. Boyde, D. Matha, V. Abel, M. Aigner, Thermodynamic process analyses of SOFC/GT hybrid systems, in: 5th International Energy Conversion Engineering Conference and Exhibit (IECEC), no. AIAA 2007-4833, 2007. doi:10.2514/6.2007-4833.

[10] Y. Yi, T. P. Smith, J. Brouwer, A. D. Rao, G. S. Samuelsen, Simulation of a 220 kw hybrid sofc gas turbine system and data comparison, in: Electrochemical Society Proceedings Volume 2003-07, 2003. doi:10.1149/200307.1442PV.

[11] Y. Ando, H. Oozawa, M. Mihara, H. Irie, Y. Urashita, T. Ikegami, Demonstration of sofc-micro gas turbine (mgt) hybrid systems for commercialization, Mitsubishi Heavy Industries Technical Review 52 (4).
URL http://www.mhi.co.jp/technology/review/pdf/e524/e524047.pdf

[12] F. Scholwin, M. Nelles, Energy flows in biogas plants: analysis and implications for plant design, in: A. Wellinger, J. Murphy, D. Baxter (Eds.), The Biogas Handbook, Elsevier, 2013, pp. 212–227. doi:10.1533/9780857097415.2.212.
URL https://doi.org/10.1533/9780857097415.2.212

[13] M. Steilen, C. Salettia, M. P. Heddrich, K. A. Friedrich, Analysis of the in influence of heat transfer on the stationary operation and performance of a solid oxide fuel cell/gas turbine hybrid power plant, Applied Energy 211 (2018) 479–491. doi:10.1016/j.apenergy.2017.11.038.
URL https://doi.org/10.1016/j.apenergy.2017.11.038

[14] European Union's Horizon 2020 research and innovation programme: Biogas-fired Combined Hybrid Heat and Power Plant (2015-2019).
URL http://www.bio-hypp.eu/

[15] N. F. Harun, D. Tucker, T. A. A. II, Impact of fuel composition transients on SOFC performance in gas turbine hybrid systems, Applied Energy 164 (2016) 446–461. doi:10.1016/j.apenergy.2015.11.031.
URL https://doi.org/10.1016/j.apenergy.2015.11.031

[16] N. F. Harun, D. Tucker, T. A. A. II, Technical challenges in operating an SOFC in fuel flexible gas turbine hybrid systems: Coupling effects of cathode air mass flow, Applied Energy 190 (2017) 852–867. doi:10.1016/j.apenergy.2016.12.160.
URL https://doi.org/10.1016/j.apenergy.2016.12.160

[17] N. F. Harun, D. Tucker, T. A. A. II, Fuel composition transients in fuel cell turbine hybrid for polygeneration applications, Journal of Fuel Cell Science and Technology 11 (6) (2014) 061001. doi:10.1115/1.4028159.
URL https://doi.org/10.1115/1.4028159

[18] L. Fryda, K. Panopoulos, E. Kakaras, Integrated CHP with autothermal biomass gasification and SOFC–MGT, Energy Conversion and Management 49 (2) (2008) 281–290. doi:10.1016/j.enconman.2007.06.013.
URL https://doi.org/10.1016/j.enconman.2007.06.013

[19] S. Wongchanapai, H. Iwai, M. Saito, H. Yoshida, Performance evaluation of a direct-biogas solid oxide fuel cell-micro gas turbine (SOFC-MGT) hybrid combined heat and power (CHP) system, Journal of Power Sources 223 (2013) 9–17. doi:10.1016/j.jpowsour.2012.09.037.
URL https://doi.org/10.1016/j.jpowsour.2012.09.037

[20] T. Krummrein, Numerical analysis of a biogas powered hybrid MGT-SOFC power plant, in: Proceedings of the 7th european fuel cell Piero Lunghi conference, no. EFC17157, 2017, pp. 267–268.
URL http://www.europeanfuelcell.it/images/proceedings_EFC17.pdf

[21] T. Krummrein, M. Henke, P. Kutne, A highly flexible approach on the steady-state analysis of innovative micro gas turbine cycles, Journal of Engineering for Gas Turbines and Power (2018, in press). doi:10.1115/1.4040855.
URL https://doi.org/10.1115/1.4040855

[22] M. Henke, T. Monz, M. Aigner, Inverted brayton cycle with exhaust gas recirculation - a numerical investigation, Journal of Engineering for Gas Turbines and Power 135 (9) (2013) 091203–1 – 091203–7. doi:10.1115/1.4024954.
URL https://doi.org/10.1115/1.4024954

[23] M. Henke, N. Klempp, M. Hohloch, T. Monz, M. Aigner, Validation of a T100 micro gas turbine steady-state simulation tool, in: Proceedings of ASME Turbo Expo 2015: Turbine Technical Conference and Exposition,GT2015-42090, June 15-19, 2015, Montreal, Canada, 2015.

[24] E. Goos, A. Burcat, B. Ruscic, Extended third millennium ideal gas and condensed phase thermochemical database for combustion with updates from active thermochemical tables (2010).
URL http://burcat.technion.ac.il/dir/BURCAT.THR

[25] J. Larminie, A. Dicks, Fuel Cell Systems Explained, 2nd Edition, Wiley, 2003.